

Hybrid Adaptive Flight Control with Bounded Linear Stability Analysis

Nhan T. Nguyen*

NASA Ames Research Center, Moffett Field, CA 94035

Maryam Bakhtiari-Nejad[†]

Perot System, NASA Ames Research Center, Moffett Field, CA 94035

Yong Huang[‡]

Clemson University, Clemson, South Carolina, SC 29634

This paper presents a hybrid adaptive control method for improving the command-following performance of a flight control system. The hybrid adaptive control method is based on a neural network on-line parameter estimation using an indirect adaptive control in conjunction with a direct adaptive control. The parameter estimation revises a dynamic inversion control model to reduce the tracking error. The direct adaptive control then accounts for any residual tracking error by a rate command augmentation. The plant parameter estimation is based on two approaches: 1) an indirect adaptive law derived from the Lyapunov direct method to ensure that the tracking error is bounded, and 2) a recursive least-squares method that minimizes the modeling error. Simulations show that the hybrid adaptive control can provide a significant improvement in the tracking performance over a direct adaptive control method alone.

I. Introduction

While air travel remains the safest mode of transportation, accidents do occur on rare occasions with catastrophic consequences. For this reason, the Aviation Safety Program under the Aeronautics Research Mission Directorate (ARMD) at NASA has created the Integrated Resilient Aircraft Control (IRAC) research project to advance the state of aircraft flight control and to provide on-board control resilience for ensuring safe flight in the presence of adverse conditions such as faults, damage, and/or upsets.¹ These hazardous flight conditions can impose heavy demands on aircraft flight control systems in their abilities to enable a pilot to stabilize and navigate an aircraft safely. The goal of the IRAC project is to arrive at a set of validated multidisciplinary integrated aircraft control design tools and techniques for enabling safe flight in the presence of adverse conditions.¹ Aircraft stability and maneuverability in off-nominal flight conditions are critical to aircraft survivability.

Adaptive flight control is identified as a technology that can improve aircraft stability and maneuverability. Stability of adaptive control remains a major challenge that prevents adaptive control from being implemented in high assurance systems such as mission- or safety-critical flight vehicles. Understanding stability issues with adaptive control, hence, will be important in order to advance adaptive control technologies. Thus, one of the objectives of IRAC adaptive control research is to develop metrics for assessing stability of adaptive flight control by extending the robust control concept of phase and gain margins to adaptive control. Another objective of the IRAC research is to advance adaptive control technologies that can better manage constraints imposed on an aircraft. These constraints are dictated by limitations of actuator dynamics, aircraft structural load limits, frequency bandwidth, system latency, and others.

The ability of an adaptive control system to modify a pre-designed flight control system is at the same time a strength and a weakness. On the one hand, the premise of being able to accommodate vehicle degradation is a major selling point of adaptive control since traditional gain-scheduled control methods are viewed to be less capable of handling off-nominal flight conditions outside their design operating points. Nonetheless, gain-scheduled control

*Computer Scientist, Intelligent Systems Division, Mail Stop 269-1, AIAA Senior Member

[†]Aerospace Engineer, Intelligent Systems Division, Mail Stop 269-1, AIAA Member

[‡]Assistant Professor, Mechanical Engineering Department, Clemson University

approaches are robust to disturbances and secondary dynamics. On the other hand, potential problems with adaptive control exist with regards to high-gain learning and unmodeled dynamics. Moreover, adaptive control algorithms can also be sensitive to other effects such as actuator dynamics, exogenous disturbances, etc.

Over the past several years, various adaptive flight control techniques have been investigated.^{2-8,10,11} Adaptive flight control provides a possibility for maintaining aircraft stability and performance by means of enabling a flight control system to adapt to system uncertainties. Research in adaptive control has spanned several decades, but challenges in obtaining robustness in the presence of unmodeled dynamics, parameter uncertainties, and disturbances as well as the issues with verification and validation still remain.^{3,13} Adaptive control laws may be divided into direct and indirect approaches. Indirect adaptive control methods are based on identification of unknown plant parameters and certainty-equivalence control schemes derived from the parameter estimates which are assumed to be their true values.¹⁵ Parameter identification techniques such as recursive least-squares and neural networks have been used in indirect adaptive control methods.⁴ In contrast, direct adaptive control methods directly adjust control parameters to account for system uncertainties without identifying unknown plant parameters explicitly. In recent years, direct model-reference adaptive control (MRAC) using neural networks has been a topic of great research interests.^{5-8,10,11} In particular, Rysdyk and Calise described a method for augmenting acceleration commands via a neural net direct adaptive control law to improve handling qualities.⁵ Johnson et al. introduced a pseudo-control hedging approach for dealing with control input characteristics such as actuator saturation, rate limit, and linear input dynamics.⁷ Idan et al. studied a hierarchical neural net adaptive control using secondary actuators such as engine propulsion to accommodate for failures of primary actuators.⁸ Hovakimyan et al. developed an output feedback adaptive control to address issues with parametric uncertainty and unmodeled dynamics.¹¹ Cao et al. developed an \mathcal{L}_1 adaptive control method to address high-gain learning.⁹

Direct MRAC based on the work by Rysdyk and Calise⁵ has been used by NASA to develop a neural net intelligent flight control system (IFCS). The IFCS has been demonstrated on an F-15 fighter aircraft.¹⁷ The intelligent flight control uses the Calise's direct MRAC, dynamic inversion control approach. The neural net direct adaption is designed to provide consistent handling qualities without requiring extensive gain-scheduling or explicit system identification. This particular architecture uses both pre-trained and on-line learning neural networks and a reference model to specify desired handling qualities. Pre-trained neural networks are used to provide estimates of aerodynamic stability and control characteristics. On-line learning neural networks are used to compensate for errors and adapt to changes in aircraft dynamics. As a result, consistent handling qualities may be achieved across different flight conditions. Recent flight test results demonstrate the potential benefits of adaptive control technology in improving aircraft flight control systems in the presence of adverse flight conditions due to failures.¹⁸ The flight test results also point out the needs for further research to increase the understanding of effectiveness and limitations of the direct adaptive flight control.

While the neural net direct adaptive law has been researched extensively and has been used with successes in a number of applications, the possibility of a high-gain control due to aggressive learning can be an issue. Aggressive learning is characterized by setting a learning rate for training a neural network high enough so as to reduce the dynamic inversion error rapidly. This can potentially lead to a control augmentation command that may saturate the control authority. A high-gain control may also excite unmodeled dynamics of the plant that can adversely affect the stability of the adaptive law. The issues with control saturation and unmodeled dynamics have been addressed by Johnson et al.⁷ and Hovakimyan et al.¹¹ but not in the context of a high-gain control. Moreover, under off-nominal flight conditions, the knowledge of plant dynamics of an aircraft may become impaired and as a result this can present a problem for a pilot to safely navigate the aircraft within a flight envelope that has been constrained by changes in aircraft flight dynamics. For example, changes in stability and control derivatives due to damage can potentially cause a pilot to apply excessive or incorrect stick commands that could worsen the aircraft handling qualities. Direct MRAC approaches accommodate changes in plant dynamics implicitly but do not provide an explicit means for ascertaining the knowledge of plant dynamics which can be used to improve adaptive control strategies by revising the plant model. Moreover, as additional side benefits, the improved knowledge of plant dynamics can potentially be used for developing fault detection isolation (FDI) strategies and emergency flight planning to provide guidance laws for safe navigation.

Another drawback with adaptive control in general is the lack of robustness in the presence of disturbances and unmodeled dynamics. In the presence of hazards such as damage or failures, flight vehicles can exhibit numerous coupled effects such as aerodynamics, vehicle dynamics, structures, and propulsion. These coupled effects impose a considerable amount of uncertainties on the performance of a flight control system. Thus, even though an adaptive control may be stable in a nominal flight condition, it may fail to maintain enough control margins in the presence of these uncertainties. For example, conventional aircraft flight control systems incorporate aeroservoelastic filters

to prevent control signals from exciting wing flexible modes. If changes in the aircraft configuration are significant enough, frequencies of the flexible modes may be shifted that render the filters ineffective. This would allow control signals to potentially excite flexible modes which can cause problems for a pilot to maintain good tracking control. Another example is the use of slow actuators such as engines as control effectors. In off-nominal events, engines are sometimes used to control aircraft. This has been shown to enable pilots to maintain control in some emergency situations such as the DHL incident involving an Airbus A300-B4 in 2003 that suffered structural damage and hydraulic loss over Baghdad,²⁰ and the Sioux City, Iowa accident involving United Airlines Flight 232.¹⁹ The dissimilar actuator rates can cause problems with adaptive control and can potentially lead to pilot-induced oscillations (PIO).²

Adaptive control methods are generally time-domain methods. Lyapunov direct method is a preferred technique for deriving stable adaptive laws which are usually nonlinear. However, robust control is usually done in the frequency domain. Robust control requires a controller to be analyzed using the phase and gain margin concepts in the frequency domain. With this tool, an adaptive control can be analyzed to assess its control margin sensitivity for different learning rates. This would then enable a suitable learning rate to be determined. By incorporating the knowledge of unmodeled dynamics, a control margin can be evaluated to see if it is sufficient to maintain stability of a flight control system in the presence of potential hazards.

In this paper, we introduce a hybrid adaptive control method that blends both direct and indirect adaptive control to improve adaptive control strategies.¹² The idea is that in the current direct MRAC approach, the dynamic inversion controller is normally based on a fixed plant model. The discrepancy between the plant model and the actual aircraft plant dynamics, called modeling error, is proportional to the tracking error dynamics. Most adaptive control approaches are designed to cancel out the effect of the modeling error. In this method, the dynamic inversion controller adapts to changes in plant dynamics by an indirect adaptive law that performs an explicit parameter estimation of plant model parameters. This results in a reduction of the modeling error that directly leads to a reduced tracking error. Any residual tracking error can then be handled by the current direct adaptive law using a smaller learning rate in order to reduce the possibility of high-gain learning.. The parameter estimation is computed using two approaches: 1) an indirect adaptive law established by the Lyapunov direct method to ensure that the tracking error is bounded, and 2) a recursive least-squares optimal estimation that minimizes the modeling error. Simulations for a damaged aircraft show that the hybrid adaptive control with the recursive least-squares indirect adaptive law can provide a significant improvement in the tracking performance over a direct adaptive control method alone.

This paper also introduces a bounded linear stability analysis for analyzing stability and convergence of adaptive control methods. Neural net adaptive control methods are generally nonlinear. However, the bounded linear stability analysis can be performed without linearizing the adaptive laws. The effect of high-gain learning for the direct MRAC and hybrid adaptive control are examined. The analysis shows the effect of learning rate on the original system gains. Moreover, the analysis also shows high frequency oscillations typically accompanied with the direct MRAC method are not significantly present with the hybrid method with the recursive least-squares indirect adaptive law. The method of bounded linear stability provides a means for assessing nonlinear adaptive control using widely available robust control analysis tools or linear systems.

II. Hybrid Adaptive Control

In an event of damage, aircraft may experience significant changes in aerodynamics and mass properties. Asymmetric damage can result in cross coupling between the longitudinal motion and lateral-direction motion. The nonlinear equations of motion for asymmetric damaged aircraft has been established.¹² To maintain stability, a rate-command-altitude hold (RCAH) controller is designed using a feedback linearization approach with true aircraft dynamics described by a linear model about its trim point in a flight envelope

$$\dot{\omega} = \dot{\omega}^* + \Delta\dot{\omega} = A_1\omega + A_2x + B\delta \quad (1)$$

where $\omega = [p \ q \ r]^\top$ is the aircraft angular rate, $x = [\alpha \ \beta \ \phi \ \delta_r]^\top$ is a trim state vector to maintain trim condition, $\delta = [\delta_a \ \delta_e \ \delta_r]^\top$ is a control vector of aileron, elevator, and rudder deflections, $A_1 \in \mathbb{R}^{n \times n}$, $A_2 \in \mathbb{R}^{n \times m}$, and $B \in \mathbb{R}^{n \times n}$ are true plant matrices which are unknown, $\Delta\dot{\omega}$ is the unknown aircraft dynamics due to parametric uncertainties, and $\dot{\omega}^*$ is the nominal aircraft dynamics described by

$$\dot{\omega}^* = A_1^*\omega + A_2^*x + B^*\delta \quad (2)$$

where A_1^* , A_2^* , and B^* are the nominal plant matrices which are assumed to be known. These matrices can generally be assumed to be associated with an ideal, undamaged aircraft.

An architecture of the hybrid adaptive control method is shown in Fig. 1. This architecture uses a reference model to specify desired handling qualities, a neural net indirect adaptive law to perform parameter estimation of true plant dynamics, a dynamic inversion controller to compute a control allocation, and a neural net direct adaptive law to compensate for any residual tracking error. The parameter estimates of the true plant dynamics are used to update the plant model used for computing the dynamic inversion controller. If the parameter estimation converges, then the modeling error is expected to reduce, thereby causing the tracking error to decrease. Any residual amount of the tracking error is then compensated for by the direct adaptive law.

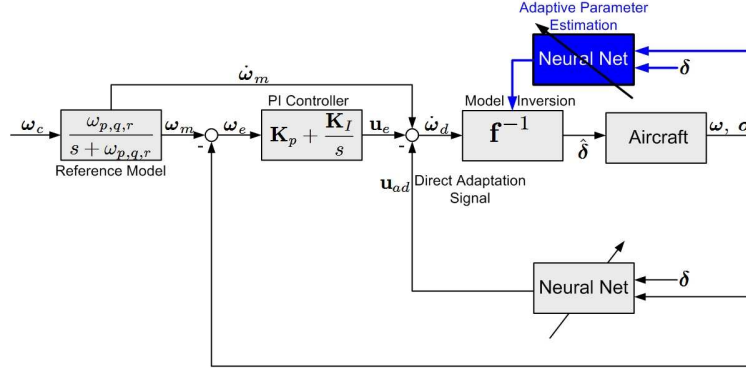


Fig. 1 - Hybrid Adaptive Flight Control Architecture

The dynamic inversion controller is computed from a plant model that is revised on-line by the indirect adaptive law according to

$$\delta = \hat{B}^{-1} (\dot{\omega}_d - \hat{A}_1 \omega - \hat{A}_2 x) \quad (3)$$

where $\dot{\omega}_d$ is the desired acceleration, and $\hat{A}_1 = A_1^* + \Delta \hat{A}_1$, $\hat{A}_2 = A_2^* + \Delta \hat{A}_2$, and $\hat{B} = B^* + \Delta \hat{B}$ are estimated plant matrices.

Because the true plant dynamics is unknown, the dynamic inversion controller will generate a modeling error

$$\varepsilon = \dot{\omega} - \dot{\omega}_d = (\Delta A_1 - \Delta \hat{A}_1) \omega - (\Delta A_2 - \Delta \hat{A}_2) x + (\Delta B - \Delta \hat{B}) \delta \quad (4)$$

where $\Delta A_1 = A_1 - A_1^*$, $\Delta A_2 = A_2 - A_2^*$, and $\Delta B = B - B^*$ are the differences between the true and nominal plant matrices. Thus, if \hat{A}_1 , \hat{A}_2 , and \hat{B} can be estimated accurately, the modeling error will be small, leading to less tracking error.

The reference model filters a pilot command r into a reference angular rate ω_m via a first-order model

$$\dot{\omega}_m = A_m \omega_m + B_m r \quad (5)$$

where $A_m \in \mathbb{R}^{n \times n}$ is Hurwitz and $B_m \in \mathbb{R}^{n \times n}$.

A tracking error signal $\omega_e = \omega_m - \omega$ is formed by comparing the reference angular rate with the actual angular rate output. The inner loop is then closed with a proportional-integral (PI) controller u_e operated on the tracking error signal as

$$u_e = K_p \omega_e + K_i \int_0^t \omega_e d\tau \quad (6)$$

where $K_p \in \mathbb{R}^{n \times n}$ and $K_i \in \mathbb{R}^{n \times n}$ are diagonal positive-definite proportional and integral gain matrices. The PI controller is designed to better handle errors detected from the angular rate feedback. A windup protection is included to limit the integrator at its current value when a control surface is saturated.

Thus, the tracking error dynamics can be expressed as

$$\dot{e} = -Ke + b(u_d - \varepsilon) \quad (7)$$

where $e = \left[\int_0^t \omega_e d\tau \quad \omega_e \right]^T$, u_d is the direct adaptive control signal, and $K \in \mathbb{R}^{2n \times 2n}$ and $b \in \mathbb{R}^{2n \times n}$ are defined as

$$K = \begin{bmatrix} 0 & -I \\ K_i & K_p \end{bmatrix} > 0, \quad b = \begin{bmatrix} 0 \\ I \end{bmatrix}$$

The eigenvalues of K are found to be as

$$\lambda(K) = \text{diag} \left[\frac{K_p}{2} \pm \left(\frac{K_p^2}{4} - K_i \right)^{\frac{1}{2}} \right] \quad (8)$$

To achieve good loop gains, the integral gain should be set such that the real part of the minimum eigenvalue is greatest. This requires

$$K_i \geq \frac{K_p^2}{4} \quad (9)$$

The system then has two complex poles in the open left half s -plane.

Referring to Eq. (7), if the direct adaptive control signal u_d or the parameter estimation from the indirect adaptive law could perfectly cancel out the modeling error ε , then the tracking error would tend to zero asymptotically. In practice, there is always some residual modeling error in the adaptation, so asymptotic stability of the tracking error is not guaranteed, but a weaker uniformly asymptotic stability could be achieved by a proper design of the direct and indirect adaptive laws.

A. Lyapunov-Based Indirect Adaptive Law

The cancellation of the modeling error is handled by the neural net indirect and direct adaptive control signals. Let

$$u_d = W_d^\top \beta_d \quad (10)$$

$$\Delta \hat{A}_1 = W_\omega^\top \beta_\omega \quad (11)$$

$$\Delta \hat{A}_2 = W_x^\top \beta_x \quad (12)$$

$$\Delta \hat{B} = W_\delta^\top \beta_\delta \quad (13)$$

where $W_d, W_\omega, W_x,$ and W_δ are neural net weights, $\beta_d, \beta_\omega, \beta_x,$ and β_δ are basis functions.

A modified single-layer sigma-pi neural network is used to model nonlinear plant parameters according to

$$\beta_d = \left[C_1 \quad C_2 \quad C_3 \quad C_4 \quad C_5 \quad C_6 \right]^\top$$

where $C_i, i = 1, \dots, 6,$ are inputs to the neural network consisting of control commands, sensor feedback, and bias terms defined as

$$C_1 = \rho_a V^2 \left[1 \quad \alpha \quad \beta \quad \alpha^2 \quad \beta^2 \quad \alpha\beta \right]$$

$$C_2 = \rho_a V^2 \omega^\top \left[1 \quad \alpha \quad \beta \right]$$

$$C_3 = \rho_a V^2 \delta^\top \left[1 \quad \alpha \quad \beta \right]$$

$$C_4 = \omega^\top \left[p \quad q \quad r \right]$$

$$C_5 = \omega^\top \left[u \quad v \quad w \right]$$

$$C_6 = \left[1 \quad \theta \quad \phi \quad \delta_T \right]$$

where $\alpha, \beta, \theta, \phi, u, v, w, V, \rho_a, \delta_T$ are angle of attack, sideslip angle, pitch angle, bank angle, forward speed, lateral speed, normal speed, absolute speed, atmospheric density, and engine throttle, respectively.

Specifically, C_1 models the aerodynamic moments due to the angle of attacks and sideslip, C_2 models the aerodynamic moments due to the angular rate, C_3 models the aerodynamic moments due to the flight control surface

deflections, C_4 models the inertial moments, and C_5 and C_6 model the inertial moments due to the center-of-gravity (CG) shift. The basis functions β_ω , β_x , and β_δ can be any suitable subset of β_d such as

$$\begin{aligned}\beta_\omega &= \rho_a V^2 \begin{bmatrix} 1 & \alpha & \beta \\ 1 & \alpha & \beta \\ 1 & \alpha & \beta \end{bmatrix}^\top \\ \beta_x &= \rho_a V^2 \\ \beta_\delta &= \beta_\omega\end{aligned}$$

The tracking error dynamics can now be written as

$$\dot{e} = -Ke + b\Phi^\top \Theta + b(u_d - \Delta\dot{w}) \quad (14)$$

where $\Phi^\top = \begin{bmatrix} W_\omega^\top & W_x^\top & W_\delta^\top \end{bmatrix}$ is a neural net weight matrix with $\Phi \in \mathbb{R}^{(2n+m) \times n}$ and $\Theta^\top = \begin{bmatrix} \omega^\top \beta_\omega^\top & x^\top \beta_x^\top & \delta^\top \beta_\delta^\top \end{bmatrix}$ is an input matrix with $\Theta \in \mathbb{R}^{2n+m}$.

The neural net weight W_d is computed by the direct adaptive law due to Rysdyk and Calise with a learning rate $\Gamma > 0$ and an e-modification parameter $\mu > 0$ ¹⁴ according to

$$\dot{W}_d = -\Gamma \left(\beta_d e^\top P b + \mu \|e^\top P b\| W_d \right) \quad (15)$$

where $\|\cdot\|$ is a Frobenius norm and $P \in \mathbb{R}^{2n \times 2n}$ solves the Lyapunov equation

$$K^\top P + PK = Q \quad (16)$$

for some positive-definite matrix Q .

Let $Q = I_{2n \times 2n}$, then solving for P in the Lyapunov equation yields

$$P = \frac{1}{2} \begin{bmatrix} K_i^{-1} K_p + K_p^{-1} (K_i + I) & K_i^{-1} \\ K_i^{-1} & K_p^{-1} (I + K_i^{-1}) \end{bmatrix} > 0$$

The e-modification term provides robustness in the direct adaptive law.¹⁴ The weight update law in Eq. (15) provides uniform boundedness of the neural net weight and the tracking error. The proof of this update law is provided by Rysdyk and Calise.⁵

The plant matrices ΔA_1 , ΔA_2 , and ΔB can be estimated using the Lyapunov direct method. The parameter estimation is given by the following normalized weight update law

$$\dot{\Phi} = -\frac{\Lambda}{m^2} \left(\Theta e^\top P b + \eta \|e^\top P b\| \Phi \right) \quad (17)$$

where $\Lambda > 0$ is a learning rate, $\eta \geq 0$ is an e-modification parameter, and $m^2 \in \mathbb{R}$ is a normalization factor defined as

$$m = 1 + \Theta^\top R \Theta \quad (18)$$

with $R \in \mathbb{R}^{(2n+m) \times (2n+m)}$ is a positive-semi-definite weight matrix. The normalization helps improve the adaptation and prevent high-gain learning.

The indirect adaptive law (17) is a stable adaptive law which can be proved as follows:

Proof: Let $W_d = W_d^* + \tilde{W}_d$ and $\Phi = \Phi^* + \tilde{\Phi}$, where the asterisk denotes the ideal weight matrices and the tilde denotes the weight deviations. The ideal weight matrices are unknown but they may be assumed constant and bounded to stay within a Δ_e -neighborhood, where

$$\Delta_e = \sup_{\beta_d} \left\| W_d^{*\top} \beta_d + \Phi^{*\top} \Theta - \Delta\dot{w} \right\|$$

Consider the following Lyapunov candidate function

$$V = e^\top P e + \text{tr} \left(\tilde{W}_d^\top \Gamma^{-1} \tilde{W}_d + \tilde{\Phi}^\top m^2 \Lambda^{-1} \tilde{\Phi} \right)$$

where $\text{tr}(\cdot)$ is a matrix trace operator.

The time derivative of the Lyapunov candidate function is then computed as

$$\begin{aligned} \dot{V} \leq & -e^\top Qe + 2e^\top Pb \left(\tilde{W}_d^\top \beta_d + \tilde{\Phi}^\top \Theta + \Delta_e \right) + 2\text{tr} \left[-\tilde{W}_d^\top \beta_d e^\top Pb \right. \\ & \left. - \mu \tilde{W}_d^\top \left\| e^\top Pb \right\| \left(W_d^* + \tilde{W}_d \right) - \tilde{\Phi}^\top \Theta e^\top Pb - \tilde{\Phi}^\top \eta \left\| e^\top Pb \right\| \left(\Phi^* + \tilde{\Phi} \right) \right] \end{aligned}$$

Completing the square yields

$$\begin{aligned} \text{tr} \left[-\tilde{W}_d^\top \mu \left\| e^\top Pb \right\| \left(W_d^* + \tilde{W}_d \right) \right] &= - \left\| e^\top Pb \right\| \left(\left\| \mu^{\frac{1}{2}} \left(\frac{W_d^*}{2} + \tilde{W}_d \right) \right\|^2 - \left\| \frac{\mu^{\frac{1}{2}} W_d^*}{2} \right\|^2 \right) \\ \text{tr} \left[-\tilde{\Phi}^\top \eta \left\| e^\top Pb \right\| \left(\Phi^* + \tilde{\Phi} \right) \right] &= - \left\| e^\top Pb \right\| \left(\left\| \eta^{\frac{1}{2}} \left(\frac{\Phi^*}{2} + \tilde{\Phi} \right) \right\|^2 - \left\| \frac{\eta^{\frac{1}{2}} \Phi^*}{2} \right\|^2 \right) \end{aligned}$$

We then obtain

$$\begin{aligned} \dot{V} \leq & -e^\top Qe + 2e^\top Pb \Delta_e - 2 \left\| e^\top Pb \right\| \left(\left\| \mu^{\frac{1}{2}} \left(\frac{W_d^*}{2} + \tilde{W}_d \right) \right\|^2 - \left\| \frac{\mu^{\frac{1}{2}} W_d^*}{2} \right\|^2 \right) \\ & - 2 \left\| e^\top Pb \right\| \left(\left\| \eta^{\frac{1}{2}} \left(\frac{\Phi^*}{2} + \tilde{\Phi} \right) \right\|^2 - \left\| \frac{\eta^{\frac{1}{2}} \Phi^*}{2} \right\|^2 \right) \end{aligned}$$

Since $\|b\| = 1$, we establish that

$$\begin{aligned} e^\top Qe &\leq \rho(Q) \|e\|^2 \\ e^\top Pb \Delta_e &\leq \rho(P) \|e\| \|\Delta_e\| \\ \left\| e^\top Pb \right\| \left\| \frac{\mu^{\frac{1}{2}} W_d^*}{2} \right\|^2 &\leq \rho(P) \|e\| \left\| \frac{\mu^{\frac{1}{2}} W_d^*}{2} \right\|^2 \\ \left\| e^\top Pb \right\| \left\| \frac{\eta^{\frac{1}{2}} \Phi^*}{2} \right\|^2 &\leq \rho(P) \|e\| \left\| \frac{\eta^{\frac{1}{2}} \Phi^*}{2} \right\|^2 \end{aligned}$$

where $\rho(Q)$ and $\rho(P)$ are the spectral radii of Q and P .

Thus, the hybrid adaptive law is uniformly asymptotically stable provided that

$$\|e\| > \frac{\rho(P)}{2\rho(Q)} \left(4\|\Delta_e\| + \left\| \mu^{\frac{1}{2}} W_d^* \right\|^2 + \left\| \eta^{\frac{1}{2}} \Phi^* \right\|^2 \right)$$

We have $\dot{e}, \Theta/m \in \mathcal{L}_\infty$, but $e \in \mathcal{L}_2$ since

$$\begin{aligned} \int_0^\infty e^\top Qe dt &\leq \rho(Q) \int_0^\infty \|e\|^2 dt \leq V(0) - V(t \rightarrow \infty) + 2\rho(P) \int_0^\infty \|e\| \|\Delta_e\| dt \\ &\quad - 2\rho(P) \int_0^\infty \|e\| \left[\left\| \mu^{\frac{1}{2}} \left(\frac{W_d^*}{2} + \tilde{W}_d \right) \right\|^2 - \left\| \frac{\mu^{\frac{1}{2}} W_d^*}{2} \right\|^2 + \left\| \eta^{\frac{1}{2}} \left(\frac{\Phi^*}{2} + \tilde{\Phi} \right) \right\|^2 - \left\| \frac{\eta^{\frac{1}{2}} \Phi^*}{2} \right\|^2 \right] dt < \infty \end{aligned}$$

This can be simplified as

$$V(t \rightarrow \infty) \leq V(0) - 2\rho(P) \int_0^\infty \|e\| \left(\left\| \mu^{\frac{1}{2}} \left(\frac{W_d^*}{2} + \tilde{W}_d \right) \right\|^2 + \left\| \eta^{\frac{1}{2}} \left(\frac{\Phi^*}{2} + \tilde{\Phi} \right) \right\|^2 \right) dt < \infty$$

Thus, the value of V as $t \rightarrow \infty$ and the tracking error e are uniformly bounded. Furthermore, if $\Delta_e = 0$, $\mu = 0$ and $\eta = 0$, we establish by means of the LaSalle-Yoshizawa theorem that $\lim_{t \rightarrow \infty} \|e\| \rightarrow 0$ so that $\|\dot{W}_d\| \rightarrow 0$ and $\|\dot{\Phi}\| \rightarrow 0$ as $t \rightarrow \infty$. This means that the indirect adaptive law will result in a convergence of the estimated $\Delta\hat{A}_1$, $\Delta\hat{A}_2$, and $\Delta\hat{B}$ to their steady state values if there is no neural network approximation error and the input signals are sufficiently rich to excite all frequencies of interest in the plant dynamics. This condition is known as a persistent excitation (PE)¹⁵

We note that the effect of the e-modification μ and η parameters is to increase the negative time rate of change of the Lyapunov candidate function so that as long as the effects of unmodeled dynamics and or disturbances do not exceed the value of $V(0)$, the adaptive signals should remain bounded. The e-modification thus makes the adaptive law robust to unmodeled dynamics.¹⁶ However, this usually comes at a sacrifice in performance as will be shown later.

□

B. Recursive Least-Squares Indirect Adaptive Law

A recursive least-squares (RLS) method can be used in lieu of the normalized Lyapunov-based indirect adaptive law (17) for identifying plant dynamics. The RLS method is an adaptive law based on the optimal estimation method that uses the modeling error as the adaptive signal instead of the tracking error as in the Lyapunov-based indirect adaptive law. The plant matrices ΔA_1 , ΔA_2 , and ΔB can be estimated as

$$\Delta\hat{A}_1 = W_\omega^\top \beta_\omega \quad (19)$$

$$\Delta\hat{A}_2 = W_x^\top \beta_x \quad (20)$$

$$\Delta\hat{B} = W_\delta^\top \beta_\delta \quad (21)$$

with the following weight update law

$$\dot{\Phi} = -\frac{1}{m}R\Theta \left(\Theta^\top \Phi - \hat{\varepsilon}^{*\top} \right) \quad (22)$$

$$\dot{R} = -\frac{1}{m}R\Theta\Theta^\top R \quad (23)$$

where $\hat{\varepsilon}^*$

$$\hat{\varepsilon}^* = \hat{\omega} - A_1^* \omega - A_2^* x - B^* \delta \quad (24)$$

is the estimated modeling error for a fixed nominal plant model which requires an estimated angular acceleration $\hat{\omega}$ as an input. Generally, the angular acceleration may not be available rate gyro sensors, but can be estimated from a Kalman filter, a differentiator, or a numerical filter via a cubic or B-spline method. In any case, the estimation of the angular acceleration will introduce an error source. If the error is unbiased, i.e., it can be characterized as a white noise about the mean value, then the RLS indirect adaptive law can be applied to estimate the changes in the plant dynamics.

The tracking error dynamics for the RLS indirect adaptive law are expressed as

$$\dot{e} = -Ke + bu_d + b \left(\Phi^\top \Theta - \varepsilon^* \right) \quad (25)$$

The proof of the RLS indirect adaptive law is as follows:

Proof: To reduce the tracking error, the modeling error must be kept minimum. The optimal estimation method can be used to minimize the modeling error. Consider the following cost least-squares functional

$$J(\Phi) = \frac{1}{2} \int_0^t \frac{1}{m^2} \left\| \Phi^\top \Theta - \hat{\varepsilon}^* \right\|^2 d\tau$$

To minimize the cost functional, we compute its gradient with respect to Φ and set it to zero, thus resulting in

$$\nabla J_\Phi^\top = \int_0^t \frac{1}{m^2} \Theta \left(\Theta^\top \Phi - \hat{\varepsilon}^{*\top} \right) d\tau = 0$$

This can be written as

$$\int_0^t \frac{1}{m^2} \Theta \Theta^\top d\tau \Phi = \int_0^t \frac{1}{m^2} \Theta \hat{\varepsilon}^{*\top} d\tau$$

Let

$$R^{-1} = \int_0^t \frac{1}{m^2} \Theta \Theta^\top d\tau$$

Then

$$R^{-1} \Phi = \int_0^t \frac{1}{m^2} \Theta \hat{\varepsilon}^{*\top} d\tau$$

Upon differentiation

$$R^{-1} \dot{\Phi} + \frac{1}{m^2} \Theta \Theta^\top \Phi = \frac{1}{m^2} \Theta \hat{\varepsilon}^{*\top}$$

and solving for $\dot{\Phi}$, the RLS indirect adaptive law is obtained as

$$\dot{\Phi} = -\frac{1}{m^2} R \Theta \left(\Theta^\top \Phi - \hat{\varepsilon}^{*\top} \right)$$

Also, we note that

$$R^{-1} \dot{R} = I \Rightarrow \dot{R}^{-1} R + R^{-1} \dot{R} = 0$$

Solving for \dot{R} yields

$$\dot{R} = -R \dot{R}^{-1} R = -\frac{1}{m^2} R \Theta \Theta^\top R$$

The RLS formula has a very similar form to the Kalman filter where Eq. (23) is a differential Riccati equation for a zero-order plant dynamics and R is called a covariance matrix. In the RLS indirect adaptive law, R acts as an adaptive learning rate with its own update law. With large enough R , the ideal product $\Phi^{*\top} \Theta$ can be shown to converge to the estimated modeling error $\hat{\varepsilon}^{*15}$ so that

$$\left\| \Phi^{*\top} \Theta - \hat{\varepsilon}^* \right\| < M$$

where $M > 0$ is some small positive constant. Then, the time derivative of the weight variation $\tilde{\Phi}$ is equal to

$$\dot{\tilde{\Phi}} = -\frac{1}{m^2} R \Theta \Theta^\top \tilde{\Phi}$$

The RLS indirect adaptive law can now be shown to be stable and result in bounded signals. Consider the following Lyapunov candidate function

$$V = e^\top P e + \text{tr} \left(\tilde{W}_d^\top \Gamma^{-1} \tilde{W}_d + \tilde{\Phi}^\top R^{-1} \tilde{\Phi} \right)$$

The time rate of change of the Lyapunov candidate function is computed as

$$\dot{V} \leq -e^\top Q e + 2e^\top P b \left(\tilde{W}_d^\top \beta_d + \tilde{\Phi}^\top \Theta + \Delta_e \right) + 2\text{tr} \left[-\tilde{W}_d^\top \beta_d e^\top P b - \mu \tilde{W}_d^\top \left\| e^\top P b \right\| \left(W_d^* + \tilde{W}_d \right) - \frac{1}{m^2} \tilde{\Phi}^\top \Theta \Theta^\top \tilde{\Phi} \right]$$

where

$$\Delta_e = \sup_{\beta_d} \left\| W_d^{*\top} \beta_d + M \right\|$$

We note that now the neural net direct adaptive law only needs to cancel out the residual recursive least-squares error which should be small enough that the learning rate does not have to be set to a large value, thereby reducing the effect of high-gain learning

Upon simplification, one obtains

$$\dot{V} \leq -e^\top Q e - 2 \left\| e^\top P b \right\| \left\| \mu^{\frac{1}{2}} \left(\frac{W_d^*}{2} + \tilde{W}_d \right) \right\|^2 - 2\text{tr} \left(\frac{1}{m^2} \tilde{\Phi}^\top \Theta \Theta^\top \tilde{\Phi} \right) \leq 0$$

Thus, the hybrid adaptive law with the recursive least-squares indirect adaptive law is stable provided that the tracking error is bounded from below by

$$\inf_{\beta_d} \|e\| = \frac{\rho(P) \|\Delta_e\|}{2\rho(Q)} \left(4\|\Delta_e\| + \left\| \mu^{\frac{1}{2}} W_d^* \right\|^2 \right)$$

□

III. Bounded Linear Stability Analysis

A key challenge with neural net adaptive flight control is to make the learning algorithm sufficiently robust. Robustness relates to the stability and convergence of the learning algorithm. Stability is a fundamental requirement of any dynamical system that ensures a small disturbance would not grow to a large deviation from an equilibrium. For systems with high assurance such as human-rated or mission-critical flight vehicles, stability of adaptive systems is of paramount importance. Without guaranteed stability, such adaptive control algorithms cannot be certified for operation in high-assurance systems. Unfortunately, the stability of adaptive controllers in general and neural net adaptive controllers in particular remains unresolved. The notion of a self-modifying flight control law using an artificial neural net learning process whose outputs may be deemed as non-deterministic is a major hurdle to overcome.

Another criterion for robustness is the convergence of the neural net learning algorithm. Neural networks are used as universal nonlinear function approximators. In the case of the adaptive flight control, the networks approximate the unknown modeling error that is used to adjust effectively the control gains to maintain a desired handling quality. Convergence requires stability and a proper design of the weight update law. It is conceivable that even though a learning algorithm is stable, the neural net weights may not converge to correct values. Thus, accurate convergence is also important since this is directly related to the flight control performance.

The neural net weight update laws in Eqs. (15), (17), and (22) are nonlinear due to the product terms involving β_d , e , Φ , and Θ . Stability of nonlinear systems is usually analyzed by the Lyapunov method. However, the concept of phase and gain margin for linear systems cannot be extended to nonlinear adaptive control. The linear control margin concept can provide understanding stability margin of adaptive control that enables more robust adaptive learning laws to be synthesized. This is only possible if the neural net weight update laws are linearized at a certain point in time with the neural net weights held constant. As adaptation occurs, the neural net weights vary with time. Hence, the time at which to freeze the neural net weights (for calculation) must correspond to a worst-case stability margin. This can be a challenge. This paper introduces a method for analyzing stability and convergence of nonlinear neural net adaptive laws using error bound analysis, which enables the dominant linear components of the nonlinear adaptive laws to be extracted from Eqs. (15), (17), and (22) without linearization of the adaptive laws at an instance in time.

A. Lyapunov-Based Direct Adaptive Law

For the direct adaptive law in Eq. (15), we note that it can be expressed as

$$\frac{d}{dt} (\beta_d^\top W_d) = -\Gamma (\beta_d^\top \beta_d e^\top P b + \mu \|e^\top P b\| \beta_d^\top W_d) + \dot{\beta}_d^\top W_d \quad (26)$$

We define an error bound on the neural net adaptive signal as

$$\Delta_{\tilde{W}_d} = \sup_{\beta_d} \left\| \tilde{W}_d^\top \dot{\beta}_d - \Gamma \mu \|e^\top P b\| W_d^{*\top} \beta \right\| \quad (27)$$

Then, the time derivative of the variation in the neural net direct adaptive signal is bounded by

$$\frac{d}{dt} (\tilde{W}_d^\top \beta_d) \leq -\Gamma (\alpha_0 \beta_d^\top P e + \mu \gamma \tilde{W}_d^\top \beta_d) + \Delta_{\tilde{W}_d} \quad (28)$$

where

$$\gamma = \sup_{\omega} \|e^\top P b\| \quad (29)$$

and $\alpha_0 > 0$ is defined as a level of persistent excitation (PE) such that the following \mathcal{L}_2 -norm PE condition is satisfied

$$\left\| \beta_d^\top \beta_d \right\| = \frac{1}{T} \int_t^{t+T} \beta_d^\top \beta_d d\tau \leq \alpha_0 \quad (30)$$

for $\beta \in \mathcal{L}_2$.

Thus, without sufficient persistent excitation and if the e-modification parameter μ is not present, the neural net weights will not necessarily converge. The persistent excitation essentially means that inputs to the neural network must be sufficiently rich in order to excite system dynamics to enable a convergence to take place.

If the error bound is small, then the linear behavior of the weight update law becomes dominant. Therefore, this enables the stability and convergence to be analyzed in a linear sense using the following equation

$$\frac{d}{dt} \begin{bmatrix} e \\ \tilde{W}_d^\top \beta_d \end{bmatrix} \leq \begin{bmatrix} -K & b \\ -\Gamma \alpha_0 b^\top P & -\Gamma \mu \gamma \end{bmatrix} \begin{bmatrix} e \\ \tilde{W}_d^\top \beta_d \end{bmatrix} + \begin{bmatrix} \Delta_e \\ \Delta_{\tilde{W}_d} \end{bmatrix} \quad (31)$$

Let A be the transition matrix. If A is negative definite, then the rate of convergence is established by the eigenvalues of A since

$$\begin{bmatrix} e \\ \tilde{W}_d^\top \beta_d \end{bmatrix} \leq e^{At} \begin{bmatrix} e(0) \\ \tilde{W}_d^\top(0) \beta_d(0) \end{bmatrix} - A^{-1} \begin{bmatrix} \Delta_e \\ \Delta_{\tilde{W}_d} \end{bmatrix} \quad (32)$$

The equilibrium is therefore uniformly asymptotically stable and converges to

$$\limsup_{t \rightarrow \infty} \begin{bmatrix} e \\ \tilde{W}_d^\top \beta_d \end{bmatrix} = \begin{bmatrix} \Delta_e \\ \Delta_{\tilde{W}_d} \end{bmatrix} \quad (33)$$

By Holder's inequality, the convergence radius can be expressed as

$$\limsup_{t \rightarrow \infty} \begin{bmatrix} e \\ \tilde{W}_d^\top \beta_d \end{bmatrix} \leq \rho(A^{-1}) \begin{bmatrix} \Delta_e \\ \Delta_{\tilde{W}_d} \end{bmatrix} \quad (34)$$

Thus, Δ_e and $\Delta_{\tilde{W}_d}$ should be kept as small as possible for the tracking error and the neural net weight matrix variation to converge as close to zero as possible.

In order to obtain a convergence, stability of the tracking error and neural net adaptive law must be established by the negative-definiteness of the eigenvalues of A . The characteristic equation of A is established by $\det(sI - A)$, which can be computed using the Schur complement

$$\det(sI - A) = (s + \Gamma \mu \gamma) \det \left[sI + K + b(s + \Gamma \mu \gamma)^{-1} \Gamma \alpha_0 b^\top P \right] \quad (35)$$

Upon expansion, the characteristic equation is obtained as

$$s^3 + K_p s^2 + K_i s + \Gamma [\mu \gamma s^2 + (\mu \gamma K_p + \alpha_0 P_{22}) s + \mu \gamma K_i + \alpha_0 P_{12}] = 0 \quad (36)$$

This equation represents the characteristic equation of the following open-loop transfer function

$$H(s) = (sI + K)^{-1} C(s) \quad (37)$$

where $C(s)$ is the transfer function of the direct adaptive control

$$C(s) = \Gamma \left[\mu \gamma s + (\mu \gamma K_p + \alpha_0 P_{22}) + \frac{\mu \gamma K_i + \alpha_0 P_{12}}{s} \right] \quad (38)$$

Thus, the direct adaptive control is a proportional-integral-derivative (PID) controller that adjusts the original proportional and integral gains K_p and K_i , as illustrated in Fig. 2.

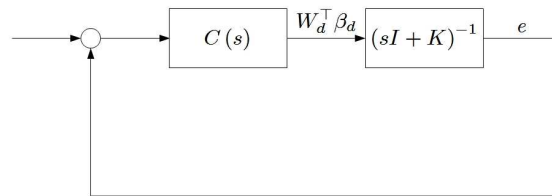


Fig. 2 - Adaptive PI Gain

The roots of the characteristic equation are the closed-loop poles which can be examined by factorization with residue. Consider the following cases:

1. If μ is small and $\mu \ll \min\left(\frac{\alpha_0 K_p^{-1} P_{22}}{\gamma}, \frac{\alpha_0 K_i^{-1} P_{12}}{\gamma}\right)$, then Eq. (36) can be factored as

$$(s + \Gamma a) [s^2 + (K_p + \Gamma \mu \gamma - \Gamma a)s + K_i + \Gamma \mu \gamma K_p + \Gamma \alpha_0 P_{22} - \Gamma a(K_p + \Gamma \mu \gamma - \Gamma a)] + r = 0 \quad (39)$$

where a and the residue r are defined as

$$a = (K_i + \Gamma \mu \gamma K_p + \Gamma \alpha_0 P_{22})^{-1} (\mu \gamma K_i + \alpha_0 P_{12}) \quad (40)$$

$$r = \Gamma (\mu \gamma K_i + \alpha_0 P_{12}) - \Gamma a [K_i + \Gamma (\mu \gamma K_p + \alpha_0 P_{22}) - \Gamma a (K_p + \Gamma \mu \gamma - \Gamma a)] \quad (41)$$

Consider two cases:

(a) For small Γ , which corresponds to slow adaptation, we see that

$$a \approx \mu \gamma + \alpha_0 K_i^{-1} P_{12} \quad (42)$$

$$r \approx 0 \quad (43)$$

Neglecting second-order terms of Γ , The approximate roots of the characteristic equation are then found to be

$$s \approx -\frac{K_p - \Gamma \alpha_0 K_i^{-1} P_{12}}{2} \pm j \left[K_i + \Gamma \alpha_0 (P_{22} - K_i^{-1} P_{12} K_p) - \frac{(K_p - \Gamma \alpha_0 K_i^{-1} P_{12})^2}{4} \right]^{\frac{1}{2}} \quad (44)$$

$$s \approx -\Gamma (\mu \gamma + \alpha_0 K_i^{-1} P_{12}) \quad (45)$$

From the complex-valued roots, the effect of the direct adaptive control is to adjust the PI gains according to

$$\bar{K}_p = K_p - \Gamma \alpha_0 K_i^{-1} P_{12} \quad (46)$$

$$\bar{K}_i = K_i + \Gamma \alpha_0 (P_{22} - K_i^{-1} P_{12} K_p) \quad (47)$$

where the bar denotes the adaptive PI gains.

The convergence radius for slow adaptation is then equal to

$$\limsup_{t \rightarrow \infty} \left\| \frac{e}{\tilde{W}_d^\top \beta_d} \right\| \leq \frac{(\mu \gamma + \alpha_0 K_i^{-1} P_{12})^{-1}}{\Gamma} \left\| \frac{\Delta_e}{\Delta_{\tilde{W}_d}} \right\| \quad (48)$$

Thus, slow adaptation results in a large convergence radius since Γ is small.

(b) For large Γ , which corresponds to fast adaptation or high-gain learning, we see that

$$\Gamma a \approx -P_{22}^{-1} P_{12} \quad (49)$$

$$r \approx -\Gamma a [K_i - \Gamma a (K_p + \Gamma \mu \gamma - \Gamma a)] \quad (50)$$

Since μ is small and Γa is finitely small even though Γ is large, then the residue r is also finitely small compared to s which is large. The approximate roots of the characteristic equation are obtained as

$$s \approx -\frac{K_p + \Gamma \mu \gamma - P_{22}^{-1} P_{12}}{2} \pm j \left\{ K_i + \Gamma [\alpha_0 P_{22} + \mu \gamma (K_p - P_{22}^{-1} P_{12})] - \frac{(K_p + \Gamma \mu \gamma - P_{22}^{-1} P_{12})^2}{4} \right\} \quad (51)$$

$$s \approx -P_{22}^{-1} P_{12} \quad (52)$$

The adaptive PI gains according to

$$\bar{K}_p = K_p + \Gamma \mu \gamma - P_{22}^{-1} P_{12} \quad (53)$$

$$\bar{K}_i = K_i + \Gamma [\alpha_0 P_{22} - \mu \gamma (K_p - P_{22}^{-1} P_{12})] \quad (54)$$

The convergence radius for high-gain learning is equal to

$$\limsup_{t \rightarrow \infty} \sup_{\beta_d} \left\| \begin{array}{c} e \\ \tilde{W}_d^\top \beta_d \end{array} \right\| \leq P_{12}^{-1} P_{22} \left\| \begin{array}{c} \Delta_e \\ \Delta_{\tilde{W}_d} \end{array} \right\| \quad (55)$$

The effect of high-learning can be discerned from the adaptive PI gains. Increasing learning causes both the K_p and K_i gain to increase accordingly. The high K_i gain will result in a high frequency oscillation in the adaptive signal.⁹ This high frequency oscillation can result in excitation of unmodeled dynamics that may be present in the system and therefore can lead to a possibility of instability since the effects of unmodeled dynamics are not accounted in the Lyapunov analysis of the neural net weight update law.¹⁵

2. If μ is sufficiently large and $\mu \gg \max\left(\frac{\alpha_0 K_p^{-1} P_{22}}{\gamma}, \frac{\alpha_0 K_i^{-1} P_{12}}{\gamma}\right)$, then the characteristic equation can be reduced to

$$s^3 + K_p s^2 + K_i s + \Gamma \mu \gamma (s^2 + K_p s + K_i) = 0 \quad (56)$$

The roots are found to be

$$s = -\frac{K_p}{2} \pm j \left(K_i - \frac{K_p^2}{4} \right)^{\frac{1}{2}} \quad (57)$$

$$s = -\Gamma \mu \gamma \quad (58)$$

The complex conjugate roots reveal that for a sufficiently large μ , the effect of learning is zero because the PI gains are reduced to their original value. Thus, increasing μ beyond a certain value can negate the potential benefits due to adaptive control. This can also be seen from the transfer function $C(s)$ where μ is the derivative gain which tends to increase damping of the tracking error response.

The convergence radius for slow adaptation is equal to

$$\limsup_{t \rightarrow \infty} \sup_{\beta_d} \left\| \begin{array}{c} e \\ \tilde{W}_d^\top \beta_d \end{array} \right\| \leq \frac{1}{\Gamma \mu \gamma} \left\| \begin{array}{c} \Delta_e \\ \Delta_{\tilde{W}_d} \end{array} \right\| \quad (59)$$

The convergence radius for fast adaptation is equal to

$$\limsup_{t \rightarrow \infty} \sup_{\beta_d} \left\| \begin{array}{c} e \\ \tilde{W}_d^\top \beta_d \end{array} \right\| \leq K_i^{-1} \left\| \begin{array}{c} \Delta_e \\ \Delta_{\tilde{W}_d} \end{array} \right\| \quad (60)$$

To illustrate the bounded linear stability analysis, a simulation was performed for a damaged twin-engine generic transport model (GTM),²² as shown in Fig. 3. A wing damage simulation was performed with 25% of the left wing missing. The neural net direct adaptive control is implemented to maintain tracking performance of the damaged aircraft. A pitch doublet maneuver is commanded while the roll and yaw rates are regulated.



Fig. 3 - Generic Transport Model

Figure 4 illustrates the effect of learning rate without the e-modification term, i.e., $\mu = 0$. Without adaptation, the performance of the flight control is very poor as significant overshoots occur. With adaptation, good tracking performance can be obtained. As the learning rate increases, the tracking error becomes smaller but high frequency signals also appear. This is consistent with the bounded linear analysis results which show that high-gain learning leads to high-frequency adaptive signals.

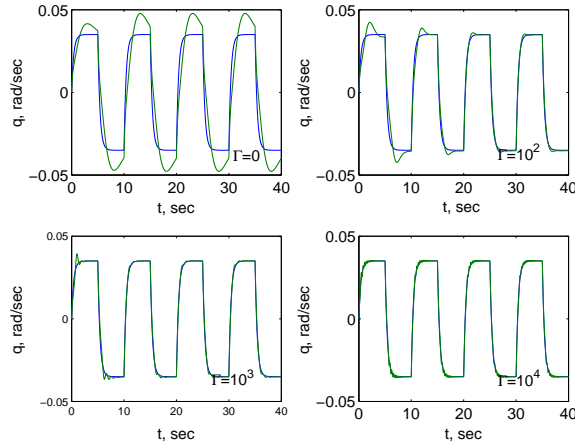


Fig. 4 - Pitch Rate Response with Direct Adaptive Law ($\mu = 0$)

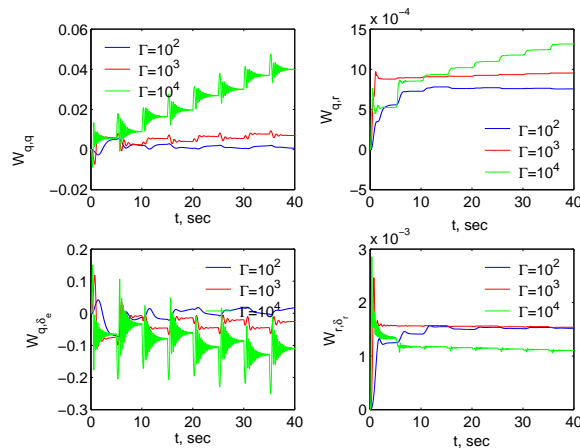


Fig. 5 - Neural Net Weight Learning with Direct Adaptive Law ($\mu = 0$)

Figure 5 is a plot of selected neural net weights for various learning rates. As can be seen, large learning rate causes high frequency oscillations in the weights. The convergence of the neural net weights $W_{q,q}$ and W_{q,δ_e} associated with linear elements q and δ_e for the pitch rate are poor. Neither of these weights would actually converge to their correct values. Thus, convergence accuracy is not demonstrated.

Figure 6 illustrates the effect of the e-modification parameter μ . As μ increases, the high-frequency amplitude reduces but the tracking error becomes worse. Eventually, with large enough value of μ , the learning essentially ceases.

Figure 7 is the plot of selected neural net weights with $\mu \neq 0$. Thus, with increasing μ , the weights are driven to zero, thereby reducing the learning of the neural network. This is consistent with the linear analysis results which show that a sufficient large μ value does not improve the adaptation. However, the reduced effectiveness of the adaptation is traded with more tolerance to unmodeled dynamics due to the e-modification scheme.

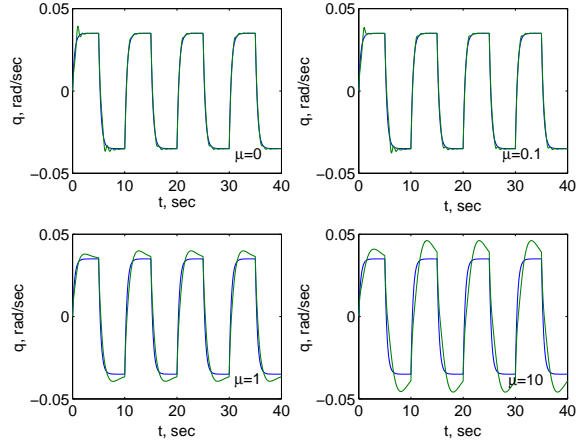


Fig. 6 - Pitch Rate Response with Direct Adaptive Law and $\mu \neq 0$ ($\Gamma = 10^3$)

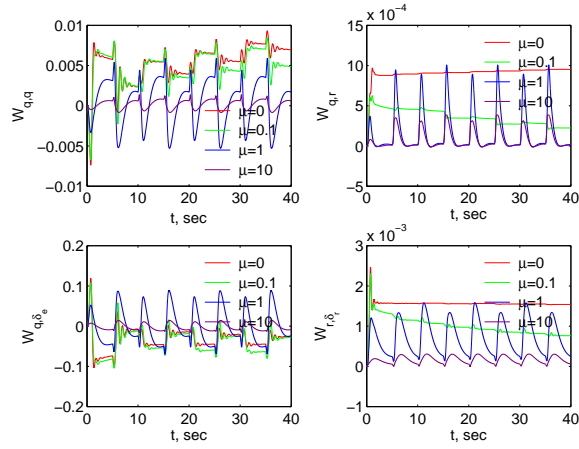


Fig. 7 - Neural Net Weight Learning with Direct Adaptive Law and $\mu \neq 0$ ($\Gamma = 10^3$)

Figure 8 is the root locus plot of the open-loop transfer function $H(s)$ for $\mu = 0$. The root locus plot agrees with the analysis by showing the high K_i gain with increasing the learning rate.

Figure 9 is the root locus plot of the open-loop transfer function $H(s)$ for $\mu = 10$. The effect of high-gain learning results in only a small change in the K_p and K_i gains according to the analysis.

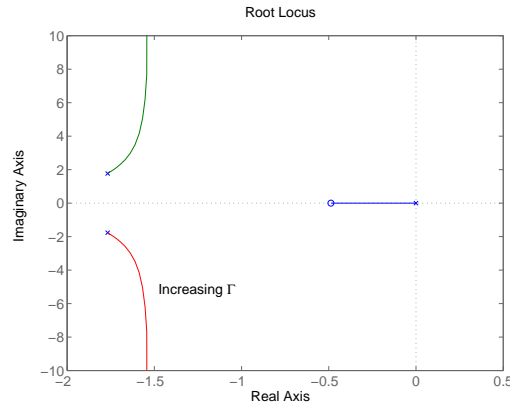


Fig. 8 - Root Locus of Pitch Axis PI Gain with Direct Adaptive Law ($\mu = 0$)

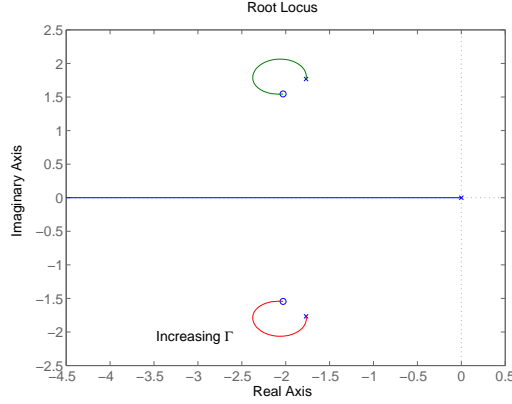


Fig. 9 - Root Locus of Pitch Axis PI Gain with Direct Adaptive Law ($\mu = 10$)

B. Lyapunov-Based Indirect Adaptive Law with Normalization

Without normalization, i.e., $R = 0$, the indirect adaptive law in Eq. (17) has a similar behavior as the direct adaptive law in Eq. (15). High-gain learning will cause a high-frequency oscillation in the parameter estimation using the Lyapunov-based indirect adaptive law. However, high-frequency oscillations can be reduced with normalization. For convenience, let $\eta = 0$ and $R \in \mathbb{R}$, Eq. (17) is equivalent to

$$\frac{d}{dt} \left(\tilde{\Phi}^\top \Theta \right) \leq -\Lambda \frac{\alpha_1}{1 + R\alpha_1} b^\top P e + \Delta \tilde{\Phi} \quad (61)$$

where $\alpha_1 > 0$ is a level of PE due to Θ

$$\left\| \Theta^\top \Theta \right\| = \frac{1}{T} \int_t^{t+T} \Theta^\top \Theta \leq \alpha_1 \quad (62)$$

The characteristic equation is obtained as

$$\det(sI - A) = s^3 + K_p s^2 + K_i s + \Lambda \frac{\alpha_1}{1 + R\alpha_1} (P_{22}s + P_{12}) = 0 \quad (63)$$

Expressing in terms of the open-loop transfer function, this is equivalent to

$$H(s) = (s^2 + K_p s + K_i)^{-1} \Lambda \frac{\alpha_1}{1 + R\alpha_1} \left(P_{22} + \frac{P_{12}}{s} \right) \quad (64)$$

The effect of adaptive control is to add a zero in the open left-half s -plane

$$s = -P_{22}^{-1} P_{12} \quad (65)$$

High-gain learning will cause the real-valued closed-loop pole to cancel this open-loop zero. The remaining complex conjugate poles are found by factorization with residue

$$s = -\frac{K_p - P_{22}^{-1} P_{12}}{2} \pm j \left[K_i + \Lambda \frac{\alpha_1}{1 + R\alpha_1} P_{22} - \frac{(K_p - P_{22}^{-1} P_{12})^2}{4} \right]^{\frac{1}{2}} \quad (66)$$

The adaptive PI gains are

$$\bar{K}_p = K_p - P_{22}^{-1} P_{12} \quad (67)$$

$$\bar{K}_i = K_i + \Lambda \frac{\alpha_1}{1 + R\alpha_1} P_{22} \quad (68)$$

If $R\alpha_1 \gg 1$, then the adaptive \bar{K}_i gain becomes

$$\bar{K}_i \approx K_i + \frac{\Lambda}{R} P_{22} \quad (69)$$

Thus, the normalization reduces the high-gain learning by a factor R , thereby attenuating high-frequency oscillations. The adaptive \bar{K}_i gain is then independent of the PE condition. However, R can not be too much larger than the learning rate Λ because it will essentially result in the adaptive \bar{K}_i gain to revert back to the original K_i gain, thereby reducing the effect of adaptation.

Figure 10 illustrates the effect of normalization on the Lyapunov-based indirect adaptive law. With no normalization and high-gain learning ($\Lambda = 10^4$), a high frequency oscillation appears in the pitch rate response. For a small value of R ($R = 10^2$), this high frequency oscillation is attenuated. However, as R increases, the tracking performance progressive worsens. When $R = \Lambda$, the tracking performance is essentially the same as that without adaptation. This observation is in good agreement with the linear stability analysis.

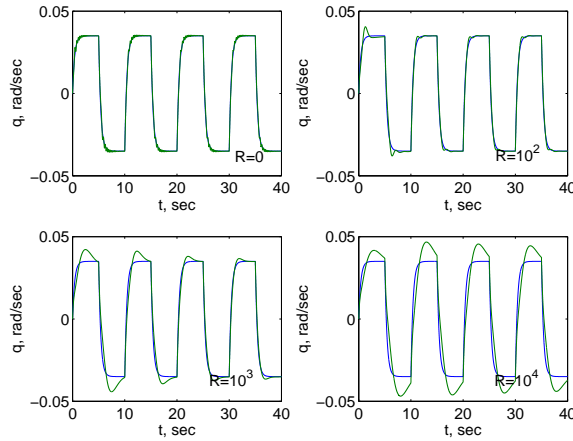


Fig. 10 - Pitch Rate Response with Normalized Lyapunov-Based Indirect Adaptive Law ($\Lambda = 10^4$)

Figure 11 is the plot of selected neural net weights with normalized indirect adaptive law. With a small value of R , the oscillations in the weights are reduced, but further increases in the value of R cause the weights to approach zero, thereby reducing the effect of learning of the neural network.

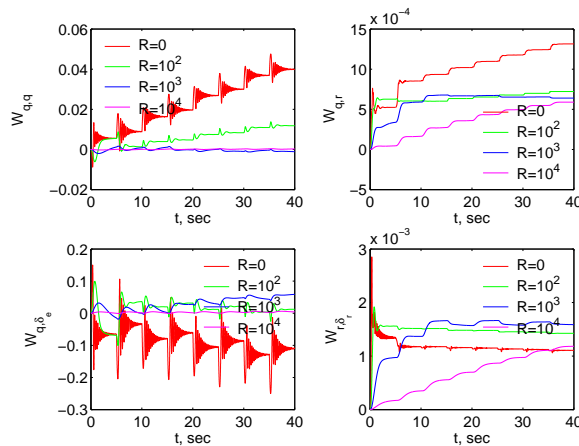


Fig. 11 - Neural Net Weight Learning with Normalized Lyapunov-Based Indirect Adaptive Law ($\Lambda = 10^4$)

Figure 12 is the root locus plot of the open-loop transfer function $H(s)$ for $R = 10^4$. Its characteristic is quite similar to non-normalized adaptive law, except that for the same learning rate, the K_i gain is not as large. The zero-pole cancellation occurs at $s = \frac{-1}{P_{22}}$ corresponding to the pitch rate.

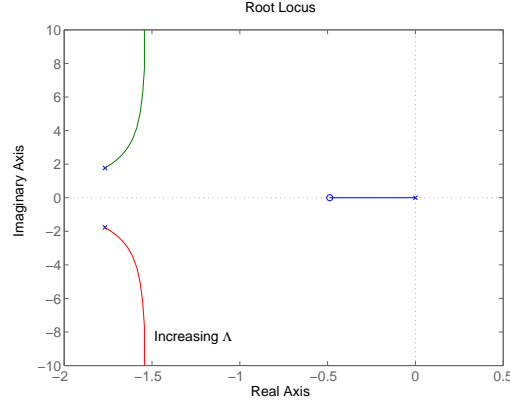


Fig. 12 - Root Locus of Pitch Axis PI Gain with Normalized Lyapunov-Based Indirect Adaptive Law ($R = 10^4$)

C. Hybrid Recursive Least-Squares Adaptive Law

The RLS indirect adaptive law is based on the optimal estimation approach rather than the Lyapunov method. The squares of the modeling error are minimized in the RLS indirect adaptive law. Using the bounded error analysis, Eq. (22) is expressed as

$$\frac{d}{dt} (\tilde{\Phi}^\top \Theta) \leq -\frac{R\alpha_1}{1+R\alpha_1} \tilde{\Phi}^\top \Theta + \Delta_{\tilde{\Phi}} \quad (70)$$

where R is a learning rate and

$$\Delta_{\tilde{\Phi}} = \sup_{\Theta} \left\| \Phi^\top \dot{\Theta} - \frac{MR\alpha_1}{1+R\alpha_1} \right\| \quad (71)$$

where $M > 0$ is a small constant equal to the convergence radius of $\Phi^{*\top} \Theta$ to the modeling error ε^* .

The Lyapunov-based direct adaptive law and the normalized Lyapunov-based indirect adaptive law are essentially the same with the only difference in the learning rate. Thus, notationally, we can simply replace $\tilde{W}_d^\top \beta_d$ with $\tilde{\Phi}^\top \Theta$. Then, the hybrid RLS adaptive law with $\mu = 0$ is described by

$$\frac{d}{dt} \begin{bmatrix} e \\ \tilde{\Phi}^\top \Theta \end{bmatrix} \leq \begin{bmatrix} -K & b \\ -\Gamma\alpha_0 b^\top P & -\frac{R\alpha_1}{1+R\alpha_1} \end{bmatrix} \begin{bmatrix} e \\ \tilde{\Phi}^\top \Theta \end{bmatrix} + \begin{bmatrix} \Delta_e \\ \Delta_{\tilde{\Phi}} \end{bmatrix} \quad (72)$$

The characteristic equation is

$$\det(sI - A) = s^3 + K_p s^2 + K_i s + \left[\frac{R\alpha_1}{1+R\alpha_1} s^2 + \left(\frac{R\alpha_1}{1+R\alpha_1} K_p + \Gamma\alpha_0 P_{22} \right) s + \frac{R\alpha_1}{1+R\alpha_1} K_i + \Gamma\alpha_0 P_{12} \right] = 0 \quad (73)$$

If $R\alpha_1 \gg 1$, then the equation is approximately equal to

$$(s+1)(s^2 + K_p s + K_i) + \Gamma\alpha_0 (P_{22} s + P_{12}) = 0 \quad (74)$$

Consider the following cases:

1. For small Γ , which corresponds to slow adaptation, the characteristic equation yields the following roots

$$s \approx -\frac{K_p}{2} \pm \left(K_i - \frac{K_p^2}{4} \right) \quad (75)$$

$$s \approx -1 \quad (76)$$

The radius of convergence is equal to

$$\limsup_{t \rightarrow \infty} \sup_{\Theta} \left\| \begin{bmatrix} e \\ \tilde{\Phi}^\top \Theta \end{bmatrix} \right\| \leq \left\| \begin{bmatrix} \Delta_e \\ \Delta_{\tilde{\Phi}} \end{bmatrix} \right\| \quad (77)$$

An interesting observation is made concerning the radius of convergence. Comparing with Eq. (48), the radius of convergence for the hybrid RLS adaptive law is independent of the learning rate. So, for a small learning rate, the radius of convergence for the Lyapunov-based direct adaptive law is large, but for the hybrid RLS adaptive law, it is finitely small. Moreover, the error bounds are not necessarily small for the Lyapunov-based direct adaptive law if convergence accuracy is not achieved. On the other hand, the RLS indirect adaptive law can be shown to provide good convergence accuracy. Therefore, the radius of convergence for the hybrid RLS adaptive law is expected to be smaller for the same small learning rate. This would mean that the Lyapunov-based direct adaptive law does not have to be a high-gain controller.

2. For large Γ , which corresponds to high-gain learning, the characteristic equation can be factored as

$$(s + \Gamma a) [s^2 + (K_p + 1 - \Gamma a)s + K_i + K_p + \Gamma \alpha_0 P_{22} - \Gamma a (K_p + 1 - \Gamma a)] + r = 0 \quad (78)$$

where for large Γ

$$\Gamma a = P_{22}^{-1} P_{12} \quad (79)$$

$$r = K_i - (K_i + K_p) P_{22}^{-1} P_{12} + (P_{22}^{-1} P_{12})^2 (K_p + 1 - P_{22}^{-1} P_{12}) \quad (80)$$

For large learning rate, r is finitely smaller than s , so the approximate roots are

$$s = -\frac{K_p + 1 - P_{22}^{-1} P_{12}}{2} \pm j \left\{ K_i + K_p - P_{22}^{-1} P_{12} (K_p + 1 - P_{22}^{-1} P_{12}) + \Gamma \alpha_0 P_{22} - \frac{(K_p + 1 - P_{22}^{-1} P_{12})^2}{4} \right\}^{\frac{1}{2}} \quad (81)$$

$$s = -P_{22}^{-1} P_{12} \quad (82)$$

The adaptive gains are

$$\bar{K}_p = K_p + 1 - P_{22}^{-1} P_{12} \quad (83)$$

$$\bar{K}_i = K_i + K_p - P_{22}^{-1} P_{12} (K_p + 1 - P_{22}^{-1} P_{12}) + \Gamma \alpha_0 P_{22} \quad (84)$$

On initial observation, we would see that high-gain learning would result in high-frequency oscillations as is the case with the Lyapunov-based direct adaptive law. However, if the convergence of the parameter estimation is achieved with the RLS indirect adaptive law, the parameter estimates then result in a dynamic inversion controller that is better matched with the true plant dynamics so that the tracking error would be nearly zero. Consequently, the resulting direct adaptive signal would be very small so that even with high-gain learning, the high adaptive K_i gain would not inject high-frequency amplitude in the tracking error.

Figure 13 illustrates the potential improvements due to the hybrid RLS adaptive law. The learning rate for the Lyapunov-based direct adaptive law is nominal ($\Gamma = 10^2$). With just a small value of R , an improvement in tracking performance can be seen. As the value of R increases, the tracking performance becomes more accurate and the pitch rate follows very closely to the reference model. No high frequency oscillation is observed with increasing the value of R , which is the learning rate for the RLS indirect adaptive law.

Figure 14 is the plot of the selected neural net weights with the hybrid RLS adaptive law. The weights exhibit a nice convergence behavior. Increasing the value of R causes the neural net weights to move closer to the true values of the system parameters for which the adaptive control is compensating. In contrast, the neural net weights in both the Lyapunov-based direct and indirect adaptive laws do not converge to their true values as shown in Figs. 5, 7, and 11. As a result, the tracking performance is not as accurate as the hybrid RLS adaptive law.

Figure 15 is the root locus plot of the transfer function for the hybrid RLS adaptive law. Increasing the learning rate causes the adaptive K_p gain to increase to its asymptotic value in Eq. (83). The K_i gain increases with high-gain Lyapunov-based direct adaptive law but with good convergence accuracy as shown in Fig. 14, high-frequency contents in the adaptive signals are expected to be well suppressed. As the learning rate increases, the real-valued closed-loop pole moves towards the open-loop zero created by the Lyapunov-based direct adaptive law. The pole-zero cancellation reduces the order of the system response to improve reference model matching in the dynamic inversion controller.

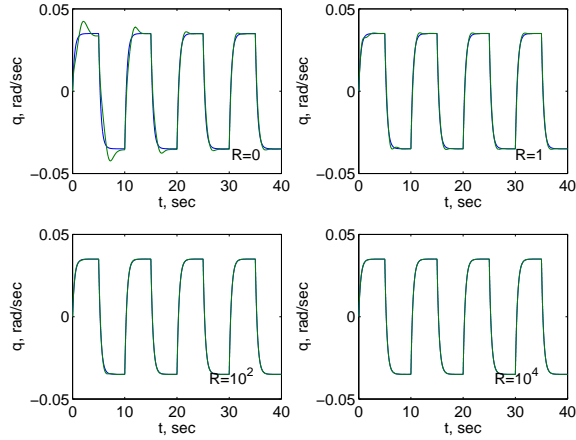


Fig. 13 - Pitch Rate Response with Hybrid RLS Adaptive Law ($\Gamma = 10^2$)

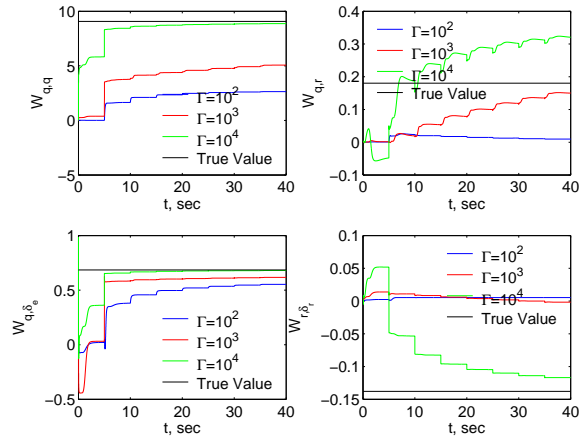


Fig. 14 - Neural Net Weight Learning with Hybrid RLS Adaptive Law

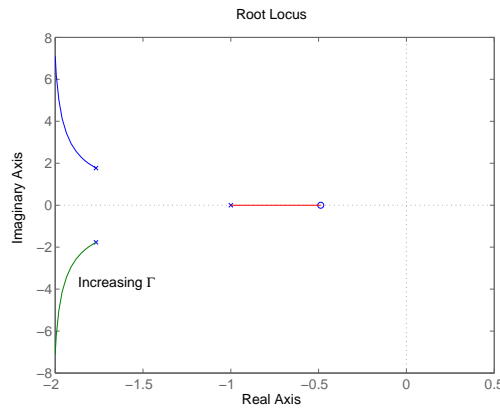


Fig. 15 - Root Locus of Pitch Axis PI Gain with Hybrid RLS Adaptive Law ($R\alpha_1 \gg 1$)

IV. Conclusions

This paper has presented a hybrid adaptive control method that blends both a direct adaptive law with an indirect direct adaptive law to improve the performance of a dynamic inversion flight controller. The indirect adaptive law is

used to perform parameter estimation to enhance the accuracy of the dynamic inversion controller so as to reduce the tracking error. Two indirect adaptive laws are presented: a Lyapunov-based method with normalization and a recursive least-squares method.

Furthermore, this paper has presented a stability and convergence analysis of these adaptive control laws. An error bound analysis has been introduced that enables linear dynamics to be extracted from the nonlinear adaptive control laws for stability and convergence analysis. The effect of the learning rate for both the existing direct adaptive law and proposed hybrid adaptive laws has been studied. Using factorization method, closed-loop poles are analyzed to demonstrate the effect of learning rate on the original controller gains. Root locus plots of the closed-loop poles are in agreement with the analytical results. With the existing direct adaptive law, high-gain learning results in an increase in the integral gain, thereby causing high-frequency oscillations in the adaptive signals. These high-frequency contents can excite unmodeled dynamics that can lead to potential destabilization of the direct adaptive law. The e-modification parameter reduces the high-frequency oscillations, but increasing this parameter further reduces the effect of adaptation. The Lyapunov-based indirect adaptive law with normalization exhibit a similar characteristic as the e-modification parameter. With small normalization factor, high-frequency oscillations can be reduced, but further increasing the normalization causes the adaptation to be less effective.

The hybrid recursive least-squares adaptive law exhibits a much better convergence accuracy than Lyapunov-based adaptive laws due to the fact that the recursive least-squares method minimizes the modeling error. In contrast, the Lyapunov-based adaptive laws only address the boundedness of the tracking error. Simulations show that the parameter estimates converge to their true values as the learning rate for the recursive least-squares indirect adaptive law increases. As a result, high-frequency oscillations are suppressed in the adaptive signals.

The bounded linear analysis provides a method for analyzing nonlinear adaptive control laws using widely available linear robust control tools. This approach represents a step towards the goal of the current research to extend the concept of linear control margins to nonlinear adaptive control. This method enables a nonlinear adaptive control to be analyzed using the concept of phase and gain margin of linear systems in the frequency domain. With this tool, an adaptive control law can be analyzed to assess its control margin sensitivity for different learning rates. This would then enable a suitable learning rate to be determined. By incorporating the knowledge of unmodeled dynamics, a control margin can be evaluated to see if it is sufficient to maintain stability of a flight control system in the presence of system uncertainties.

References

- ¹Totah, J., Krishnakumar, K., and Vikien, S., "Integrated Resilient Aircraft Control - Stability, Maneuverability, and Safe Landing in the Presence of Adverse Conditions", NASA Aeronautics Research Mission Directorate Aviation Safety Program, April 13, 2007.
- ²Steinberg, M.L., "A Comparison of Intelligent, Adaptive, and Nonlinear Flight Control Laws", AIAA Guidance, Navigation, and Control Conference, AIAA-1999-4044, 1999.
- ³Rohrs, C.E., Valavani, L., Athans, M., and Stein, G., "Robustness of Continuous-Time Adaptive Control Algorithms in the Presence of Unmodeled Dynamics", IEEE Transactions on Automatic Control, Vol AC-30, No. 9, pp. 881-889, 1985.
- ⁴Eberhart, R.L. and Ward, D.G., "Indirect Adaptive Flight Control System Interactions", International Journal of Robust and Nonlinear Control, Vol. 9, pp. 1013-1031, 1999.
- ⁵Rysdyk, R.T. and Calise, A.J., "Fault Tolerant Flight Control via Adaptive Neural Network Augmentation", AIAA Guidance, Navigation, and Control Conference, AIAA-1998-4483, 1998.
- ⁶Kim, B.S. and Calise, A.J., "Nonlinear Flight Control Using Neural Networks", Journal of Guidance, Control, and Dynamics, Vol. 20, No. 1, pp. 26-33, 1997.
- ⁷Johnson, E.N., Calise, A.J., El-Shirbiny, H.A., and Rysdyk, R.T., "Feedback Linearization with Neural Network Augmentation Applied to X-33 Attitude Control", AIAA Guidance, Navigation, and Control Conference, AIAA-2000-4157, 2000.
- ⁸Idan, M., Johnson, M.D., and Calise, A.J., "A Hierarchical Approach to Adaptive Control for Improved Flight Safety", AIAA Journal of Guidance, Control and Dynamics, Vol. 25, No. 6, pp. 1012-1020, 2002.
- ⁹Cao, C., Patel, V.V., Reddy, C.K., Hovakimyan, N., Lavretsky, E., and Wise, K., "Are Phase and Time-Delay Margin Always Adversely Affected by High Gains?", AIAA Guidance, Navigation, and Control Conference, AIAA-2006-6347, 2006.
- ¹⁰Idan, M., Johnson, M.D., Calise, A.J., and Kaneshige, J., "Intelligent Aerodynamic/Propulsion Flight Control For Flight Safety: A Nonlinear Adaptive Approach", American Control Conference, Arlington, VA, June 2001.
- ¹¹Hovakimyan, N., Kim, N., Calise, A.J., Prasad, J.V.R., and Corban, E.J., "Adaptive Output Feedback for High-Bandwidth Control of an Unmanned Helicopter", AIAA Guidance, Navigation and Control Conference, AIAA-2001-4181, 2001.
- ¹²Nguyen, N., Krishnakumar, K., Kaneshige, J., and Nespeca, P., "Dynamics and Adaptive Control for Stability Recovery of Damaged Asymmetric Aircraft", AIAA Guidance, Navigation, and Control Conference, AIAA-2006-6049, 2006.
- ¹³Jacklin, S.A., Schumann, J.M., Gupta, P.P., Richard, R., Guenther, K., and Soares, F., "Development of Advanced Verification and Validation Procedures and Tools for the Certification of Learning Systems in Aerospace Applications", Proceedings of Infotech@aerospace Conference, Arlington, VA, Sept. 26-29, 2005.

¹⁴Narendra, K.S. and Annaswamy, A.M., "A New Adaptive Law for Robust Adaptation Without Persistent Excitation", IEEE Transactions on Automatic Control, Vol. AC-32, No. 2, pp. 134-145, 1987.

¹⁵Ioannu, P.A. and Sun, J. *Robust Adaptive Control*, Prentice-Hall, 1996.

¹⁶Lewis, F.W., Jagannathan, S., and Yesildirak, A., *Neural Network Control of Robot Manipulators and Non-Linear Systems*, CRC, 1998.

¹⁷Williams-Hayes, P.S., "Flight Test Implementation of a Second Generation Intelligent Flight Control System", Technical Report NASA/TM-2005-213669.

¹⁸Bosworth, J. and Williams-Hayes, P.S., "Flight Test Results from the NF-15B IFCS Project with Adaptation to a Simulated Stabilator Failure", AIAA Infotech@Aerospace Conference, AIAA-2007-2818, 2007.

¹⁹National Transportation Safety Board, "United Airlines Flight 232 McDonnell-Douglas DC-10-10, Sioux Gateway Airport, Sioux City, Iowa, July 19, 1989", NTSB/AAR90-06, 1990.

²⁰Lemaignan, B., "Flying with no Flight Controls: Handling Qualities Analyses of the Baghdad Event", AIAA Atmospheric Flight Mechanics Conference, AIAA-2005-5907, 2005.

²¹Gilbreath, G.P., "Prediction of Pilot-Induced Oscillations (PIO) due to Actuator Rate Limiting Using the Open-Loop Onset Point (OLOP) Criterion", M.S. Thesis, Air Force Institute of Technology, Wright-Patterson Air Force Base, Ohio, 2001.

²²Bailey, R.M, Hostetler, R.W., Barnes, K.N., Belcastro, C.M., and Belcastro, C.M., "Experimental Validation: Subscale Aircraft Ground Facilities and Integrated Test Capability", AIAA Guidance, Navigation, and Control Conference, AIAA-2005-6433, 2005.